INDIGENOUS POLYCYCLIC AROMATIC HYDROCARBONS IN CIRCUMSTELLAR GRAPHITE GRAINS FROM PRIMITIVE METEORITES

S. MESSENGER,[1] S. AMARI, X. GAO, AND R. M. WALKER

McDonnell Center for the Space Sciences and Physics Department, Washington University, One Brookings Drive, St. Louis, MO 63130;
srm@nist.gov, sa@howdy.wustl.edu, xg@howdy.wustl.edu, rmw@howdy.wustl.edu

S. J. CLEMETT, X. D. F. CHILLIER,[2] AND R. N. ZARE

Department of Chemistry, Stanford University, Stanford, CA 94305; simon@d31rz3.stanford.edu, chillier@ssa1.arc.nasa.gov,
rnz@d31rz3.stanford.edu

AND

R. S. LEWIS

Enrico Fermi Institute, University of Chicago, 5630 Ellis Avenue, Chicago, IL 60637; royl@rainbow.uchicago.edu

ABSTRACT

We report the measurement of polycyclic aromatic hydrocarbons (PAHs) in individual circumstellar graphite grains extracted from two primitive meteorites, Murchison and Acfer 094. The $^{12}C/^{13}C$ isotope ratios of the grains in this study range from 2.4 to 1700. Roughly 70% of the grains have an appreciable concentration of PAHs (500–5000 parts per million [ppm]). Independent *molecule-specific* isotopic analyses show that most of the PAHs appear isotopically normal, but in several cases correlated isotopic anomalies are observed between one or more molecules and their parent grains. These correlations are most evident for ^{13}C-depleted grains. Possible origins of the PAHs in the graphite grains are discussed.

Subject headings: circumstellar matter — dust, extinction — ISM: molecules — molecular processes — stars: carbon

1. INTRODUCTION

Several kinds of refractory circumstellar grains have been found preserved in primitive meteorites (Anders & Zinner 1993). These grains are known to have an extrasolar origin on the basis of their extremely anomalous isotopic compositions. Circumstellar grains isolated to date include silicon carbide (Bernatowicz et al. 1987; Tang & Anders 1988), silicon nitride (Hoppe et al. 1994; Nittler et al. 1995), graphite (Amari et al. 1990; 1993a), corundum (Huss et al. 1994; Nittler et al. 1994), diamonds (Lewis et al. 1987), and Ti, Ti-Zr-Mo, and Fe carbides (Bernatowicz et al. 1991). With the exception of diamonds, whose mean size is ~ 16 Å (Carey et al. 1987), and the refractory carbides, which are found only as small ~ 20 nm inclusions in graphite grains, individual grains can be measured for their isotopic composition.

These circumstellar grains come from a variety of isotopically distinct stellar sources. Isotopic analysis has been used to determine their probable stellar origins, which include C- and O-rich asymptotic giant branch (AGB) stars, supernovae, and possibly novae and Wolf-Rayet stars. It is often possible to perform isotopic analyses of both major and minor elements, providing detailed constraints on stellar nucleosynthesis models. Transmission electron microscopy (TEM) studies of circumstellar graphite grains have recently been used to provide information on the temperature, pressure, and chemical composition of the stellar atmospheres from which the grains condensed (Bernatowicz et al. 1996). Here we extend the range of measurements to include the identification of isotopically correlated, and hence indigenous, organic molecules in circumstellar graphite grains.

The molecules measured in this study, polycyclic aromatic hydrocarbons (PAHs), represent an important class of organic molecules that are believed to be abundant and widely distributed throughout the cosmos. PAHs have been identified in carbonaceous and ordinary chondrites (Hahn et al. 1988; Zenobi et al. 1989; Clemett et al. 1992; Zenobi et al. 1992), interplanetary dust particles (Clemett et al. 1993; Thomas et al. 1995), and the reducing atmospheres of outer solar system bodies (Sagan et al. 1993).

PAHs are among the few molecular species capable of surviving the harsh ultraviolet (UV) radiation environment of the diffuse interstellar medium. They are considered to be the best candidates responsible for the unidentified infrared (UIR) emission features (Leger & Puget 1984; Allamandola, Tielens, & Barker 1985) observed in a variety of astrophysical environments including planetary nebulae (Cohen et al. 1986), reflection nebulae (Geballe et al. 1985), H II regions (Bregman et al. 1989), and galactic nuclei (Willner et al. 1977). Interstellar PAHs have been estimated to make up 3%–15% of the cosmic C, based on the strength of the infrared (IR) emission features (Allamandola et al. 1989).

Neutral, radical, and/or ionized PAHs may also be carriers of the diffuse interstellar bands (DIBs) (Salma et al. 1996 and references therein). DIBs are a family of broad absorption features superposed on the interstellar extinction curve. Well over 100 such bands have been identified, varying considerably in strength and shape. Positive identification of PAHs as carriers of some of the DIBs is likely to be extremely difficult owing to the complex variability in the shapes, positions, and relative strengths of these features along different lines of sight.

While there appears to be abundant evidence for aromatic compounds in the interstellar medium, spectroscopic methods are generally limited to detecting gas phase molecules in UV-rich environments and provide little information on what specific compounds are present. Because of

---

these limitations, PAH formation mechanisms and chemistry in interstellar or circumstellar regions remain uncertain. In this work we report the identification of specific PAH molecules likely formed in the circumstellar environments that also produced the circumstellar graphite grains found in primitive meteorites.

2. EXPERIMENTAL TECHNIQUES

2.1. *Sample Preparation*

Circumstellar graphite grains represent an extremely small fraction ($\lesssim 1$ part per million [ppm]; Amari, Lewis, & Anders 1994) of the meteorites that contain them. Isolation of the graphite is achieved through a series of chemical digestion steps and physical separations that successively destroy specific mineral phases while enriching graphite in the resulting meteoritic residue (Amari et al. 1994). Most of the mass of the parent meteorite is in the form of silicates ($\sim 96\%$), which are destroyed by HF/HCl acid treatments. Sulfur-bearing phases ($\sim 1\%$ of the meteorite) are removed by treatment with organic solvents and KOH. Kerogen ($\sim 2\%$ of the meteorite) is removed by a combination of $Cr_2O_7^{-2}$ and H_2O_2. Diamonds (~ 600 ppm) are separated from the residue by forming a colloid at $pH \sim 11$ by adding 0.1M $NH_3 \cdot H_2O$. Graphite grains are extracted from the remaining residue (now representing $\sim 0.2\%$ of the original meteorite) through a density separation followed by a size separation ($> 1 \mu m$).

Although greatly enriched in abundance, circumstellar graphite still represents a small part (0.1%–30%) of the final density separate from which the grains are extracted. Nevertheless, previous work has shown that circumstellar graphite grains have distinct morphologies (spherical with a platy "onion" or knobby "cauliflower" appearance) that allow them to be identified among numerous other phases (Amari, Zinner, & Lewis 1993b). Small aliquots of the graphite separate were dispersed on Au foil for examination by scanning electron microscopy/energy dispersive X-ray analysis (SEM/EDX). Candidate grains were selected on the basis of high C content (as determined by EDX) and morphological features characteristic of Murchison (CM2) circumstellar graphite. Although the distinctive appearance of circumstellar graphite grains serves as a useful tool for their identification, isotopic analysis is required to distinguish grains that are demonstrably of circumstellar origin from those that are isotopically normal and may have a solar system origin.

A total of 124 spherical graphite grains were chosen from acid residues of four primitive chondrites. The grains ranged in size from 3 to 6 μm in diameter. Most of the grains (105) came from two residues of the Murchison CM2 chondrite; 15 of which were selected from the KFC1 density separate (2.15–2.20 g cm^{-3}) prepared at the University of Chicago (Amari et al. 1994). All other residues were prepared at Washington University, including 90 grains from a Murchison separate (MKE2: density range 2.0–2.3 g cm^{-3}), five grains from the unique meteorite Acfer 094 (Newton et al. 1995), six grains from the enstatite chondrite Indarch (E4), and eight grains from the unequilibrated ordinary chondrite Tieschitz (H3).

All candidate grains were individually transferred to a sputter-cleaned Au substrate. While observing with a 100 × binocular optical microscope, each grain was picked from the residue by employing a dry W needle with a 1 μm tip attached to a micromanipulator. Once transferred, the grains were crushed into the Au substrate with a spectroscopic grade, clean quartz disk in order to increase their surface area and improve their contact with the mount surface.

Grains were measured for the presence of PAHs by two-step laser desorption laser ionization mass spectrometry (μL^2MS) as described below. Following the organic analysis, 89 of the grains were measured for their bulk C-isotopic composition using the Washington University modified Cameca IMS-3f ion microprobe mass spectrometer. This measurement sequence was chosen to avoid the possibility that the ion probe measurements would affect the PAHs present.

The techniques for making C- and N- isotopic measurements by ion microprobe have been described by Zinner, Tang, & Anders (1989).

2.2. *μL^2MS Technique*

The μL^2MS technique (Kovalenko et al. 1992; Clemett & Zare 1997) combines the advantages of laser desorption to volatilize intact neutral molecules from a solid sample with the molecular selectivity and sensitivity of resonance-enhanced multiphoton ionization (REMPI) and the high ion transmission, unlimited mass range, and multichannel detection of a reflectron time of flight (RTOF) mass spectrometer.

In the first step, constituent molecules of a circumstellar grain are desorbed with a pulsed IR laser beam focused on a 35 μm spot using a Cassegrainian microscope objective. The laser power is kept low to minimize decomposition and assure that only neutral species are desorbed. In the second step, the desorbed molecules are selectively ionized with a UV laser beam and extracted into an RTOF mass spectrometer.

One of the main advantages of using a laser photoionization process is that one can choose conditions that give rise to species-selective ionization. In this study a $(1 + 1)$ REMPI scheme was used, where absorption of one UV photon causes a PAH molecule to make a transition to its first excited electronic singlet state ($S_0 \rightarrow S_1$) and absorption of a second UV photon causes ionization. Selectivity in ionization results from the UV photon energy being resonant with the transition to an intermediate excited state, because the ionization efficiency for resonant ionization is greater by many orders of magnitude than that of nonresonant multiphoton processes (Pappas et al. 1989). Hence only those molecules in resonance with the UV laser wavelength are appreciably ionized. Because nearly all PAHs have a high photon absorption cross section at a wavelength of 266 nm associated with electronic excitation of the aromatic ring ($\pi \rightarrow \pi^*$), this procedure provides a highly selective ionization window for PAHs. Furthermore, this ionization process causes negligible fragmentation of the PAH species because there is very little rotational and vibrational excitation (Winograd, Baxter, & Kimock 1982; Shibanov 1985) acquired during the ionization event. Consequently, the mass spectra obtained by the μL^2MS instrument are easily interpreted since observed mass peaks overwhelmingly reflect parent ion species.

2.3. *μL^2MS Analysis Procedure*

The Au substrate on which several individual circumstellar grains are crushed is placed on a brass sample mount and introduced into the μL^2MS instrument through a

vacuum interlock. After introduction into the main vacuum chamber, samples are left to outgas for about 15 minutes or until the pressure in the main chamber returns to the original base pressure of less than 5×10^{-8} torr.

The sample platter is positioned just below the extraction region of the RTOF mass spectrometer and brought into the focus of the Cassegrainian microscope objective using an x-y-z manipulator. For sample viewing, a macro zoom lens is used in a telescope mode so that an image of each grain to be analyzed can be projected onto a CCD video camera. To couple the video camera to the microscope objective, a 2 mm thick Ge flat is used, which reflects visible light used for sample viewing but transmits the IR light of the desorption laser. The sample is illuminated from the exterior to the vacuum chamber through a side viewport with a focused quartz halogen lamp, which is incident at a glancing angle.

IR light from a pulsed CO_2 laser (Alltec AL 853: 10.6 μm, 120 ns FWHM with a 4 μs tail) is attenuated and beam shaped using a variable high-power (Venetian blind/spatial filter) attenuator similar to that described by Bialkowski (Bialkowski 1987). The beam is then collimated and clipped before entering the vacuum chamber with two collimating irises opened to a diameter equal to that of the microscope spider mirror (5 mm) and then focused with the reflecting microscope objective (Ealing $\times$ 36) into a 35 μm diameter spot on the sample. The laser pulse energy is chosen to maximize the desorption yield without producing appreciable fragmentation or ionization. The typical pulse energy is 22 μJ, with $\sim$ 5.2 μJ contained in the initial spike and $\sim$ 16.8 μJ in the tail. The pulse shape depends on the CO_2 laser gas mixture. The gas mixture of 68.6% He, 18% N_2, 9% CO_2, 4% CO, and 0.4% H_2 used in these experiments provides the most stable operation; shot-to-shot fluctuations in the peak intensity of the laser profile are less than 10%. To find the laser power providing the optimal PAH desorption yields from grains, a standard sample platter with fragments of Allende (CV3) matrix ($\sim$ 100 μm average diameter) pressed onto KBr was used. The IR laser power density is estimated to be $\sim$ 2.5 $\times$ 10^6 W cm^{-2}, and this value is representative of power densities for all grains discussed in this study.

After an appropriate time delay (25 μs), the fourth harmonic of a pulsed Nd:YAG laser (Spectra Physics DCR11: 266 nm, 2.5 ns FWHM fast pulse mode with a Gaussian mode output coupler) is attenuated with a half waveplate–calcite polarizer combination, apertured to a 1 mm diameter with an iris, and directed between the center electrodes of the modified Wiley-McLaren (Wiley & McLaren 1955) ion extraction region. The ionization laser pulse energy is chosen to maximize parent ion signal intensities produced by (1 + 1) REMPI with minimal fragmentation; a typical pulse energy is $\sim$ 2 mJ, giving a UV laser power density of $\sim$ 1.25 $\times$ 10^6 W cm^{-2}. The ions produced by the UV laser are extracted from the source and injected into an RTOF mass spectrometer. The reflectron geometry greatly improves the mass resolution ($t/2\,\Delta t \sim 1500$) essential for molecular isotopic analysis. To enhance ion transmission to the detector, the ion trajectories are controlled with an Einzel lens and two sets of deflection plates before injection into the reflectron. The total flight path length is 3 m. A 20 cm^2 active area dual microchannel plate detector with an oversized anode (Galileo TOF-4000) is used in a Chevron configuration to detect the ions; the output passes through

a fast preamplifier (LeCroy VV100BTB: 500 Mhz bandwidth) and a timing filter (Ortec 474 timing/filter amp) and is displayed on a 350 MHz digital oscilloscope (LeCroy 9450). As an internal reference, a metered leak valve is used to introduce a constant background of perdeuterotoluene ($^{12}C_7^2H_8$) as a reference gas. This enables periodic optimization of the ion collection optics and aids in mass calibration.

2.4. Confidence in PAH Mass Identifications

Several independent lines of evidence show that peaks in the μL^{2}MS spectra of circumstellar grains originate predominantly or exclusively from PAHs. First, the nature of the ionization process used for μL^{2}MS, (1 + 1) REMPI, is highly selective toward PAHs (Clemett 1996 and references therein). The photoionization cross sections of PAHs at the wavelength of 266 nm are many orders of magnitude higher than other organic or inorganic species (Zenobi & Zare 1991 and references therein), with only a few notable exceptions such as the alkali metals, e.g., K and Na, which are efficiently ionized by a one-photon process. Second, while in principle it is possible that there are unknown and previously unobserved inorganic or nonaromatic organic species in sufficient abundance to appear in the μL^{2}MS spectra, this possibility is considered extremely unlikely in the results presented here. The circumstellar graphite grains measured in this study are $\sim$97.5% C, $\sim$2.4% N, and $\sim$0.1% H by weight, and hence inorganic (non–C-bearing) species can be present at only trace abundance. Thirdly, the grains have been extracted from their parent meteorites by harsh chemical digestion processes, involving both strong acids and oxidizing conditions, which less chemically resilient organic species are unlikely to survive. Finally, the measurement of the exact mass of a peak can be used as an independent method for verifying its assignment as an aromatic species. The molecular weights of all PAHs have small excesses relative to integer atomic numbers. For example, the exact mass of phenanthrene ($^{12}C_{14}^1H_{10}$) is 178.0780 atomic mass units (amu) compared with that based on integer atomic weights of 178 amu. The reason arises from variations in nuclear binding energies; the exact mass of ^{1}H is $\sim$1.0078 amu relative to the mass of ^{12}C, which is by definition 12.0000 amu. All other elements have mass *deficits* relative to ^{12}C, with the exception of He, Li, Be, B, N, Th, and U. As a result, with a few exceptions, only hydrocarbon species show mass excesses. Assuming that the mass excess in a peak occurs principally from H, which has the largest mass excess per unit mass of any element, quantification of this excess provides a means to estimate the number of H atoms in that molecular species.

Consider the molecule phenanthrene. This species has been independently detected in the Murchison meteorite (Pering & Ponnamperuma 1971; Levy, Grayson, & Wolf 1973), and thus a peak of mass 178 amu in the μL^{2}MS analysis of bulk Murchison can be reasonably assumed to arise from phenanthrene. Figure 1 shows the accurate mass-calibrated μL^{2}MS spectrum in the region about 178 amu for a small particle of Murchison matrix. The exact mass of the 178 amu peak is found to be 178.078 amu, a value in precise agreement with the calculated exact mass of phenanthrene. The agreement in the observed mass excess excludes the possibility of inorganic species. Figure 2 represents the result of applying this *mass difference analysis* to other known parent PAHs and their alkylated homologs in
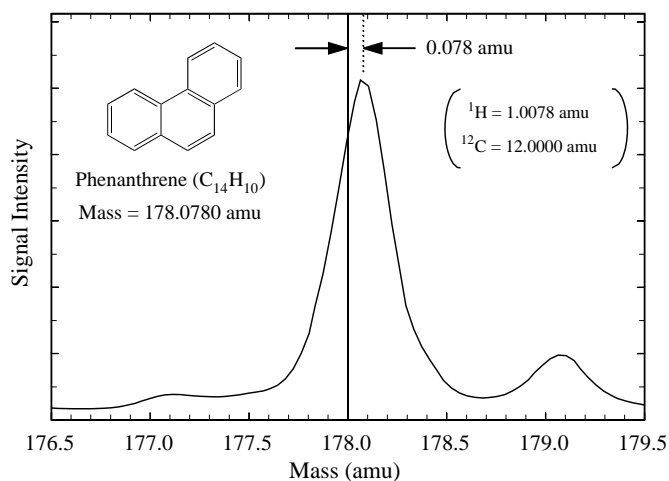
FIG. 1.—Mass spectrum of Murchison matrix obtained by the $\mu L^2 MS$ technique about the mass region 178 amu. The large peak at mass 178.078 amu is phenanthrene ($^{12}C_{14}{}^1H_{10}$). The small mass excess of 0.078 amu from 178.000 amu is caused by the slight mass excess of ^1H (1.0078 amu).

Murchison. Excellent agreement is observed in all cases between calculated mass excesses and those experimentally measured.

Extensive $\mu L^2 MS$ measurements of carbonaceous standards, including pyrolytic graphite and graphite square weave fabric, have demonstrated that PAHs are not formed in situ from laser desorption in the $\mu L^2 MS$ instrument. While PAHs may be produced at high desorption power densities, at and beyond the plasma ignition threshold, these are conditions that are never used in $\mu L^2 MS$ measurements. The reasons for this are threefold: First, selectivity in ionization is lost since the desorption process indiscriminately generates ions. Second, only low mass resolution spectra can be obtained since the high density of charged species leads to Coulombic repulsion in the desorption plume allowing both ions and neutral species (through collisions) to acquire high kinetic energies. This leads to poor mass resolution since the Wiley-McLaren/reflectron geometry of the $\mu L^2 MS$ instrument provides only space focusing and not energy focusing. Thirdly, since ions generated in the desorption plume are formed prior to the UV
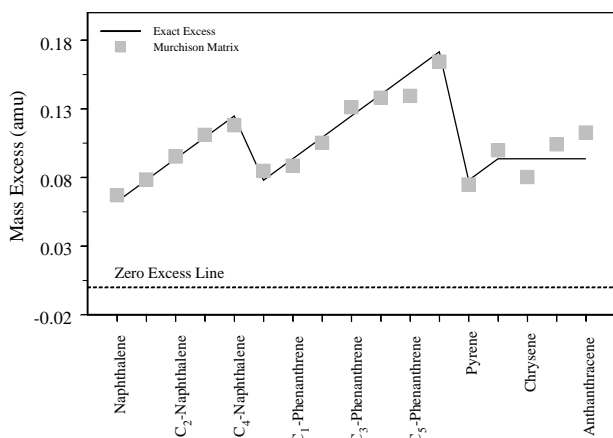

FIG. 2.—Comparison of the exact and measured mass excesses for the dominant PAH species observed in Murchison matrix. The close agreement between measured and calculated mass excess justifies mass assignment as PAH species.

laser ionization they are not correctly mass calibrated and thus lead to signal artifacts. Hence, the PAHs observed from circumstellar grains are not artifacts of the measurement process and truly reflect species present in the grains at the time of measurement.

2.5. Molecular Isotopic Measurements

Any hydrocarbon measured by $\mu L^2 MS$ has $n + 1$ mass peaks in which n is the number of C atoms in the molecule. The substitution of ^2H for ^1H can be neglected owing to the extremely low cosmic abundance of ^2H ($^2H/^1H \sim 1.5 \times 10^{-5}$). Each mass peak (isotopomer) represents a different number of ^{12}C and ^{13}C atoms in the molecule. The relative abundance of the various isotopomers follows a simple binomial distribution

$$(a + b)^n = a^n + na^{n-1}b + \frac{n(n-1)a^{n-2}b^2}{2!} + \cdots, \quad (1)$$

where a is the fractional abundance of ^{12}C, b is the abundance of ^{13}C, and n is the number of C atoms in the molecule. For solar isotopic composition $a = 0.989$ and $b = 0.011$. In this expansion, the first term represents the relative abundance of the "parent" peak (^{12}C atoms only), the second term gives the relative abundance of the first isotopomer peak (one ^{13}C substitution), and so forth.

In solar system materials ($^{12}C/^{13}C \sim 89$) for $n \lesssim 89$ the most abundant molecules observed will contain only ^{12}C atoms, with heavier isotopomers occurring in decreasing abundance. For instance, the PAH pyrene ($C_{16}H_{10}$) has 17 isotopomers. For an isotopically normal sample, the most abundant molecule is $^{12}C_{16}H_{10}$, while a smaller fraction is $^{12}C_{15}{}^{13}C_1H_{10}$ and a still smaller fraction is $^{12}C_{14}{}^{13}C_2H_{10}$. In isotopically normal samples heavier isotopomers are usually below detection limits.

Because the ^{12}C to ^{13}C ratio R is given by a/b, the R-value of a given molecule can be determined from the ratio of the intensity of any two isotopomer peaks, provided that the number of C atoms in the molecule is also known. Thus, given sufficient signal strength and minimal spectral crowding it is possible to determine the C-isotopic composition of individual molecules in a PAH mass spectrum. The technique of molecule-specific isotopic analysis by $\mu L^2 MS$ is described in detail by Maechling, Clemett, & Zare (1995).

Molecule-specific isotopic analysis begins with assigning a given mass peak to a known PAH species, thereby determining the number of C atoms in the molecule. The number of C atoms in the molecule and the intensity of the parent peak are used to calculate the "expected" intensity of the first isotopomer peak, assuming isotopically normal C. The measured intensity of the isotopomer peak is then compared with the expected value.

In practice, however, PAH spectra contain a complex mixture of aromatic species, many of which overlap each other at the mass resolution of the $\mu L^2 MS$ instrument. For instance, the parent peak of phenanthridine ($^{12}C_{13}H_9N$: 179.073 amu) cannot be resolved from the first isotopomer peak of phenanthrene ($^{12}C_{13}{}^{13}C_1H_{10}$: 179.082 amu). Such chemical interferences are indistinguishable from excesses in the first isotopomer peak, compromising the identification of ^{13}C-rich molecules. However, chemical interferences only cause ^{13}C-poor molecules to appear more isotopically normal. Stated in another way, we can be more confident about the measurement of ^{13}C depletion than about ^{13}C enrichment.

As a self-consistency check, Figure 3 shows the molecule-specific isotope ratio measurements for the five most abundant parent PAH species (naphthalene: $C_{10}H_8$; phenanthrene: $C_{14}H_{10}$; pyrene: $C_{16}H_{10}$; chrysene: $C_{18}H_{12}$; benzopyrene: $C_{20}H_{12}$) and their alkylated homologs from 11 meteorite acid residues (CI, CM, L, LL, and H classes). All the residues have normal C isotope ratios and contain complex mixtures of aromatic species whose $\mu L^2 MS$ spectra have intensities and distributions comparable to those observed from the individual grains in this study. The integrated peak intensity of the ^{12}C isotopomer peak is plotted against that of the first ^{13}C isotopomer peak. In such a plot, molecules of solar isotope composition lie along a diagonal line whose slope is R_{solar}. From Figure 3 this behavior is seen to be a limiting case with a spread in the data that appears to indicate ^{13}C enrichment relative to solar. The cause of this effect has been discussed above, from heteroaromatic species and fragmentation, both of which can contribute to the intensity of the first ^{13}C isotopomer peak. However, apparent ^{13}C depletions *cannot* be produced by such interferences, and no indication of ^{13}C

depleted PAHs exists in the spectra of any of the bulk acid residues beyond the statistical uncertainties associated with measurement effects at the weak signal limit.

2.6. *Confidence in Molecular Isotope Measurements*

Concurrent with the PAH analysis of circumstellar grains, extensive checks were performed to ascertain the confidence with which experimental molecule-specific isotopic measurements could be made. C isotope ratios for the three deuterated PAHs, toluene-$^1H_8(C_7^1H_8)$, toluene-$^2H_8(C_7^2H_8)$, and *meta*–xylene-$^2H_{10}(C_8^2H_{10})$ were measured over a wide range of signal intensities, bracketing the range observed from the grains in this study. The role of mass discrimination effects was accurately quantified in isotope determination. These PAHs were specifically chosen because they could be conveniently introduced into the $\mu L^2 MS$ instrument through a calibrated leak valve and have masses that are atypical of those observed in the spectra of circumstellar grains. Hence, residual traces of these PAHs, which can typically reside in the chamber for several days after introduction, did not provide any chemical interferences in the analysis of grain spectra. Additionally, each of the isotope references was independently analyzed with a commercial high-precision isotope mass spectrometer. The results are summarized by Maechling et al. (1995) and indicate that although the $\mu L^2 MS$ instrument is currently unable to distinguish between subtle isotope variations produced by chemical isotopic fractionation ($R_{solar} \pm 3$), it is able to resolve clearly the anticipated large nucleosynthetic C isotope variations ($R = 2$–6000) of any PAHs indigenous to circumstellar graphite grains.

3. RESULTS

Of the 89 graphite grains measured by ion microprobe mass spectrometry, 38 were found to be ^{13}C poor, and 20 were found to be ^{13}C rich relative to the solar system value; see Figure 4. The C-isotopic ratios R of these grains range from 2.4 to 1700. These values lie well outside the range of solar system materials ($R = 89$–93), demonstrating the extrasolar origin of these grains. The remaining 31 grains, including all grains from the Tieschitz and Indarch meteor-
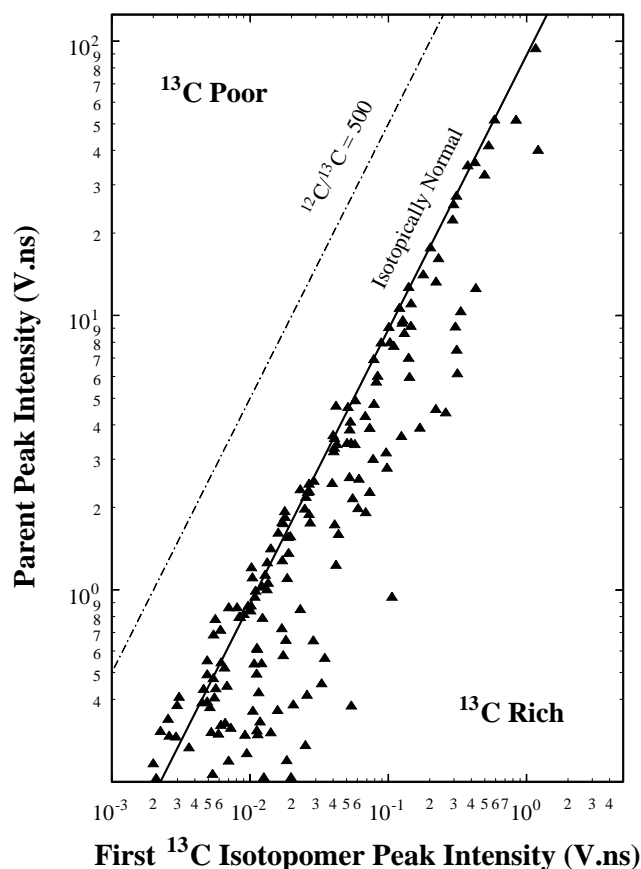
FIG. 3.—Molecular isotope analysis of PAH molecules from 11 bulk acid residues (CI, CM, L, LL, and H petrologic classes). All the residues have bulk C isotope ratios that are normal, i.e., $R = 89$. The integrated signal intensity of the ^{12}C parent peak is plotted against the integrated signal intensity of the first ^{13}C isotopomer peak divided by the number, n, of carbon atoms in the molecular species (e.g., $n = 14$ for phenanthrene). On such a plot the data should fall on a line whose slope is 89. From the plot it is clear that R-values fall on the line and off to the ^{13}C-rich region of the graph. The latter spread is an inevitable result of chemical interferences and instrumental measurement effects. However, none of the molecules measured in this study appear significantly depleted in ^{13}C, demonstrating that ^{13}C depletions are not observed by the $\mu L^2 MS$ technique on isotopically normal materials.
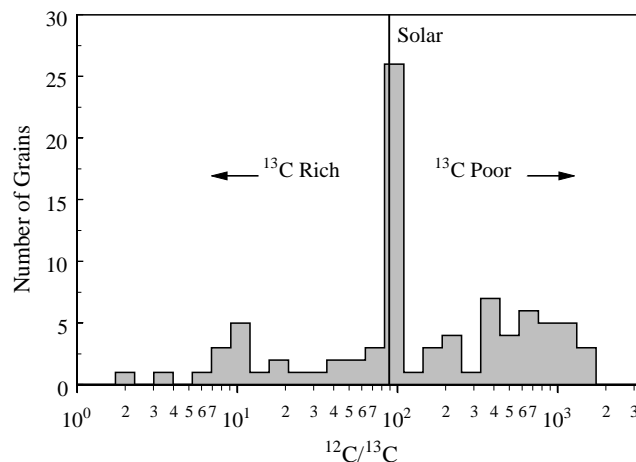
FIG. 4.—Bulk carbon-isotopic measurements of the 89 grains measured by ion microprobe mass spectrometry. The range of $^{12}C/^{13}C$ observed among the grains in this study (2.4–1720) agrees well with previous analyses of circumstellar graphite in meteorites. The strong peak centered about the solar value includes the 14 normal grains measured from the Tieschitz and Indarch meteorites.

ites, have C-isotopic compositions indistinguishable from the solar value. The fact that all candidate grains from Tieschitz and Indarch are isotopically normal is consistent with previous work that has shown circumstellar graphite to be in very low abundance in Tieschitz and as yet unknown in Indarch.

Of the 124 grains studied by $\mu L^2 MS$, 86 grains had PAH concentrations that were equal to or greater than Murchison bulk (HF-HCl) acid residue, i.e., ~ 1000 ppm. The estimated concentration of PAHs in Murchison bulk acid residue (composed primarily of PAHs and macromolecular material) is based on their abundance in bulk Murchison of 15–28 ppm (Cronin et al. 1988) and the relative concentration factor in the residue of ~ 37 (Clemett 1996).

In general, these grains were found to have extensive suites of PAHs, spanning the mass range from 100 to 600 amu, containing both parents and alkylated homologs. The spectra show a variety of aromatic species, with large variations in both signal strength and mass distribution among the grains (see Fig. 5). Large variations persist when the grains are subdivided into those with light, heavy, and normal C. Although the dominant PAH species observed in the bulk Murchison meteorite (naphthalene, pyrene, phenanthrene, and benzopyrene; Clemett 1996) are also present in most grains, substantial grain-to-grain differences exist in the relative abundance of these molecules. In comparison to bulk Murchison or its acid residue, the mass distributions of PAHs observed among the grains show higher complexity and include a larger proportion of high molecular weight species (>250 amu). The extreme variability in the PAHs observed among the grains strongly argues against a pervasive laboratory contaminant or production of the PAH species during the chemical digestion process used to prepare the residues from which the grains were isolated. Furthermore, PAHs present in meteoritic acid residues differ only slightly from those in untreated bulk meteorite samples, as illustrated in Figure 6. The primary effect of the acid treatments appears to be partial destruction of more labile species, *not* PAH production. We conclude that the observed molecules resided with their parent graphite grains in their meteorite parent bodies.
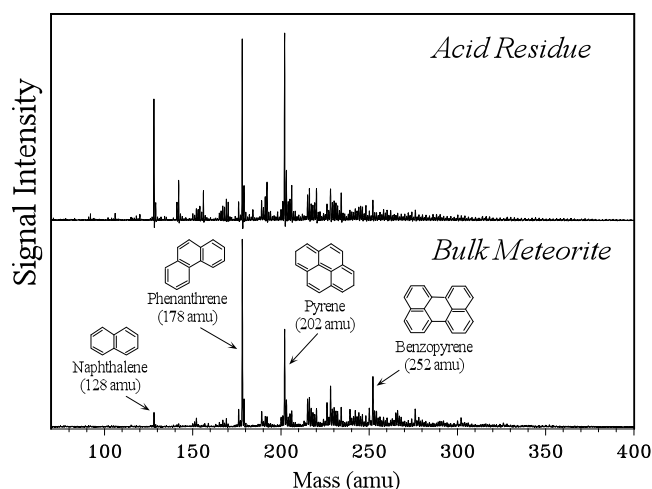
FIG. 6.—$\mu L^2 MS$ spectra of the PAHs in bulk Murchison and its acid residue (EKG 11.11.86). Each spectrum is independently scaled and comparison of signal intensities are valid only within each spectrum. The increase in low-mass PAHs in the acid residue is attributed to the acid residue procedure, however, no new peaks are observed and the residue preparation is considered to have only a minimal impact on the native PAH distribution.

C_{60} (720 amu) and related fullerenes and fulleranes have been postulated to be potential major constituents of carbonaceous material produced in circumstellar outflows (Kroto et al. 1985; Kroto 1988). The $\mu L^2 MS$ instrument is capable of detecting the presence of such species, albeit at lower detection sensitivities than that for PAHs (Clemett 1996). No evidence exists in any of the grains analyzed in this study for the presence of C_{60} or related species in circumstellar graphite. This finding does not, however, preclude their presence at concentrations below current detection limits (~ 500 ppm) and/or their destruction during the chemical and physical treatments used to extract the grains from their parent meteorite.

All molecular peaks with sufficient signal intensity and minimal spectral crowding were subjected to isotopic analysis. Many grain spectra had peak densities too high to permit isotopic analysis, with heteroaromatic species and/or fragmentation peaks overlapping with isotopomer peaks of interest. Somewhat less than one-third of the peaks with sufficient signal strength were also free of obvious interferences, limiting our isotopic measurements to 85 peaks from 13 ^{13}C-poor grains and 30 peaks from 6 normal grains. See § 2.5 for a discussion of molecular isotopic measurements.

The limited number of total counts $(n_1 + n_2 = N)$ making up the parent (n_1) and first isotopomer peaks (n_2)—typically 50–200 counts—makes it necessary to determine whether an apparent isotopic anomaly is due simply to a statistical fluctuation. We choose to approach this issue by assessing the likelihood that a given molecule represents a sample of isotopically normal material. However, because the sample size (N) is very small, the relative probabilities of observing different proportions of N ions in the parent and first isotopomer peaks follows a binomial (asymmetric) rather than a Gaussian probability distribution. This makes it necessary to calculate the probability distribution for each molecular isotopic measurement.

The relative probability of observing n_1 ions in the parent peak and n_2 ions in the first isotopomer peak, given a
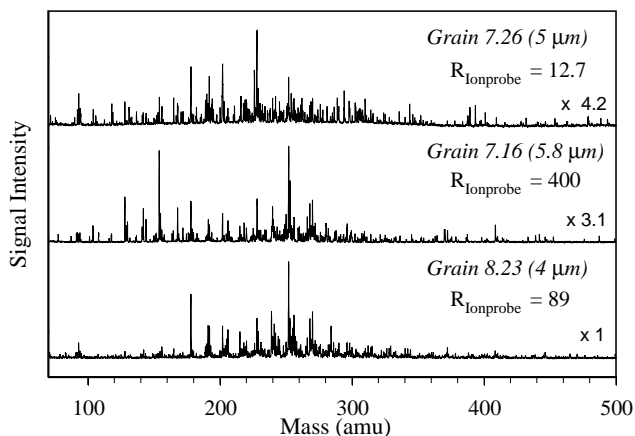

FIG. 5.—Mass spectra of the PAH distributions observed in heavy, normal, and light C grains illustrating the molecular diversity of PAHs observed with the $\mu L^2 MS$ technique. The vertical scales of the spectra from grains 7.16 and 7.26 are expanded relative to that of grain 8.23, by factors of 3.1 and 4.2, respectively.

sample of $n_1 + n_2 = N$ ions from an isotopically normal reservoir, is given by the binomial theorem

$$P_N(n_1) = \frac{N!}{n_1! \, n_2!} \, p_1^{n_1} p_2^{n_2} \, , \qquad (2)$$

where p_1 and p_2 are the relative probabilities of observing an ion in the first and second peak, respectively. The relative probabilities of observing a parent ion and a first isotopomer peak ion are given by the first two terms of the binomial expansion, as discussed in § 2.5. We determine the probability distribution for a given molecule by calculating the probabilities of observing different proportions of the (total observed) N ions in the first two isotopomer peaks, from $n_1 = N$ and $n_2 = 0$ to $n_1 = 0$ and $n_2 = N$. An example of a probability distribution derived in this way is shown in Figure 7a. The resultant distribution is asymmetric, falling off more gradually for apparent ^{13}C excesses than for apparent ^{13}C depletions.

A given isotopomer distribution generally falls outside of some confidence interval centered about the most likely isotopomer distribution for an isotopically normal sample. By integrating the probability distribution over this confidence interval, we can assess the likelihood of observing a particular isotopomer distribution. As an example, the molecule phenanthrene in the isotopically normal grain M8.23 has 195 ions in the parent peak (178 amu) and 19 ions in the first isotopomer peak (179 amu). The most likely distribution for $N = 214$ (195 + 19) ions from an isotopically normal reservoir is found to be $n_1 = 185$ and $n_2 = 29$. Thus, in this case, the confidence interval extends from $n_2 = 20$ to $n_2 = 38$, where $P_{N=214}$ $(n_2 = 20) \lesssim P_{N=214}$ $(n_2 = 38)$. We find that 94% of all observations fall within this confidence interval, and thus the probability of observing this particular isotopomer distribution from an isotopically normal reservoir is less than 6%. This example represents the lowest probability isotopomer distribution we observed among all molecules analyzed from isotopically normal grains and

meteorite acid residues. However, a limited number of such low-probability events are expected to be observed from an isotopically normal reservoir, given the number of observations performed. Hence, we find no evidence of ^{13}C depleted molecules occurring in isotopically normal grains beyond expected levels of statistical fluctuations.

Most peaks from graphite grains with light C also appear isotopically normal. However, approximately five peaks from four grains appear significantly depleted in ^{13}C, beyond the variations expected from isotopically normal materials given the number of measurements performed. In the most extreme case, illustrated in Figure 7b, the molecule C_2-phenanthrene in grain M7-20 ($R = 648$) has 136 ions in the parent peak (206 amu) and 7 ions in its first isotopomer peak (207 amu), where 24 are expected for a solar $^{12}C/^{13}C$ ratio. The probability of observing this distribution for an isotopically normal sample is approximately three chances in 10,000 (0.0003). Clearly such an observation is very unlikely to be the result of statistical fluctuations, given the limited number (85) of measurements performed. For two additional cases, the probabilities of observation $[P_N(n_2) = 0.0035, 0.0018]$ are again well below what one would expect to observe in a normal sample given the number of observations. In one notable case, two low-probability distributions are observed within a single grain, M11.15 ($R = 1727$). It is interesting to note that these two molecules, phenanthrene $[P_N(n_2) = 0.038]$ and C_1-phenanthrene $[P_N(n_2) = 0.012]$, may share a genetic relationship, both representing part of an alkylation series of phenanthrene. The likelihood of observing two such low-probability distributions within the same grain is extremely low. Considered together, these observations provide a compelling case for the presence of an isotopically anomalous PAH component in some circumstellar graphite grains.

The isotopic analyses of all molecules measured from normal and light C graphite grains are summarized in Figure 8. Most molecules measured in both isotopically normal grains and those with ^{13}C depletions are consistent
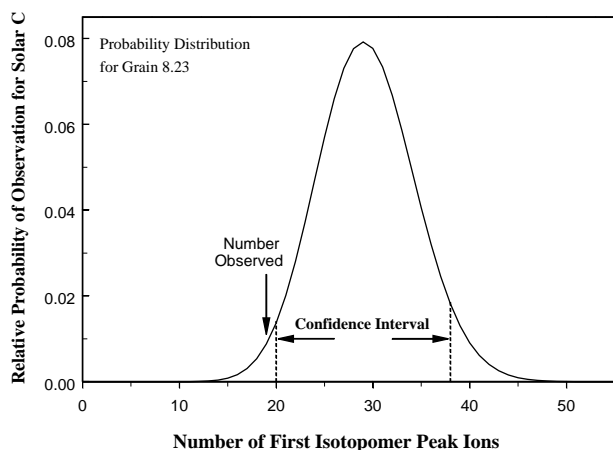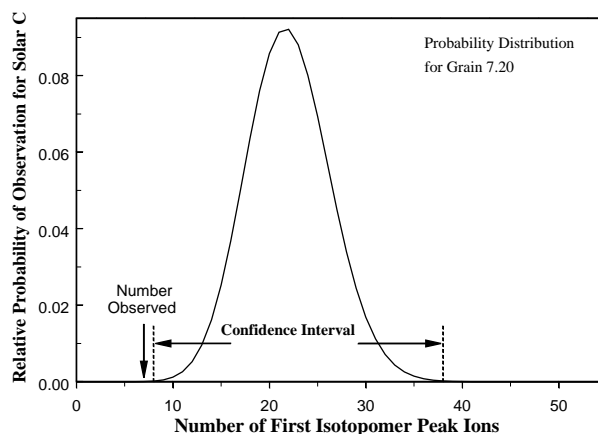
FIG. 7a

FIG. 7b

FIG. 7.—(a) Probability distribution calculated for the molecule phenanthrene in grain M8.23. The distribution represents the probability of observing a range of relative numbers of ions in the parent (n_1) and first isotopomer peak (n_2) for this molecule from an isotopically normal reservoir given the total number of ions actually measured. In this case, the probability that this molecule has a solar $^{12}C/^{13}C$ ratio is estimated by integrating the probability distribution from $n_2 = 20$ to $n_2 = 38$, which have equivalent relative probabilities of observation. This integration takes into account the asymmetricity of the distribution, which becomes pronounced as the total number of ions observed is reduced. This confidence interval includes roughly 94% of all observations, which indicates that the observed isotopomer distribution occurs less than 6% of the time in isotopically normal materials. Since ~30 peaks were measured in normal grains, this distribution can be explained by expected statistical fluctuations. (b) Probability distribution for the molecule C_2-phenanthrene in grain M7-20. Unlike the example given in Fig. 7a, the confidence interval here is 99.97%, and thus it is very unlikely (.0003) that this molecule has a solar C-isotopic composition.
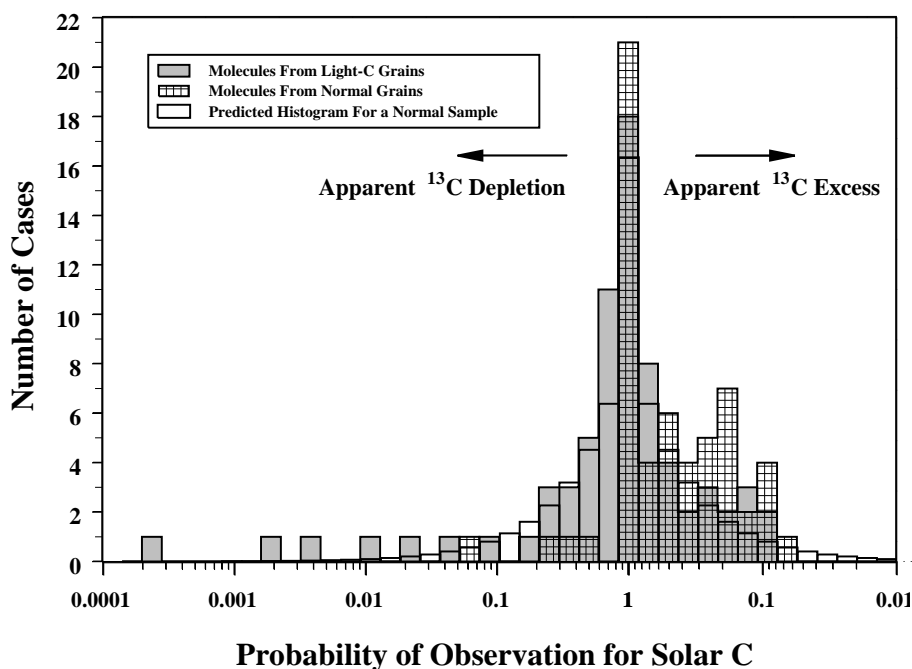
Fig. 8.—Summary of the isotopic analysis of all molecules measured in isotopically normal and ^{13}C-poor grains. The histograms illustrate the relative probabilities that the analyzed molecules are isotopically normal, as described in the text. The histogram drawn with a solid line shows the predicted frequency of observation of these events in the given probability intervals. The probability histogram for molecules from isotopically normal grains is strongly shifted to the ^{13}C-rich side of the predicted histogram. This apparent bias toward ^{13}C-rich molecules has resulted from isobaric interferences. This shift is not apparent in the probability histogram for molecules from ^{13}C-poor grains, possibly indicating that many molecules from these grains are ^{13}C-poor but are masked by minor isobaric interferences. Several molecules from ^{13}C-poor grains appear strongly depleted in ^{13}C, well beyond expected statistical fluctuations.

with being isotopically normal, within expected statistical variations. Chemical interferences lead to apparent ^{13}C excesses in some cases and likely cause both distributions to be somewhat more ^{13}C rich than their intrinsic values. Indeed, the distribution observed for molecules from normal C grains and meteoritic acid residues is strongly shifted toward higher ^{13}C abundances than expected. It is interesting to note that the distribution observed for molecules from ^{13}C-poor grains is not biased in this way. One explanation for this difference is that the molecules observed from ^{13}C-poor graphite grains are free from any molecular interferences. However, given that the spectral complexity observed among these grains is at least as rich as that observed among normal C grains and meteoritic acid residues, it is more likely that a substantial portion of the molecules measured are ^{13}C poor but are masked by isobaric interferences and an isotopically normal component. Indeed, in most cases only a few ions arising from chemical interferences would be sufficient to obscure a ^{13}C depletion.

As discussed in § 2.4, the validity of the molecular identification, and therefore the isotopic analysis, can be tested by measuring the precise mass of a given peak. Because precise mass measurements rely on the peaks in question being well formed, it was not possible to apply this additional criterion to many of the grain spectra owing to the relatively low signal strengths. Nevertheless, for most of the molecules subject to isotopic analysis, the peaks were sufficiently strong to resolve the predicted mass excesses. Figure 9 shows the deviations from integer atomic mass for molecules from normal C grains whose PAH signals were strong enough to permit precise mass determinations. In all cases mass excesses are observed, and the scatter in the data

forms a normal distribution about the predicted values. Figure 9 also shows mass excesses determined for molecules identified as depleted in ^{13}C. Again all these molecules exhibit mass excesses, strongly indicating that the species are hydrocarbons.

The identification of ^{13}C-rich molecules on grains is complicated, as discussed earlier, by interferences perturbing the actual isotopomer peak distribution. Isotopic analysis does become feasible, however for very ^{13}C-rich molecules that appear in uncongested spectral regions. This is because the intensity distribution of the isotopomer peaks is now no longer concentrated in the first and second peaks but rather is dispersed over multiple isotopomer peaks, all with appreciable intensity. By way of illustration, Figure 10 demonstrates the calculated isotopomer distribution for the molecule phenanthrene at three values of R, chosen to span the range of those observed among the grains in this study. Thus in a spectral region where there is little evidence for interference peaks, an extended isotopomer distribution associated with a particular molecule is unlikely to be caused by chemical interference because it would likely have an impact on only one or two isotopomer peaks. Hence, it is statistically improbable that a chemical interference would affect the entire isotopomer distribution or that it would correctly mimic the expected isotopomer distribution for that grain.

In the mass spectrum of grain M7.25 ($R = 18$), a strong mass peak is observed at 154 amu and is assigned to the PAH species acenaphthalene ($C_{12}H_{12}$). Figure 11 shows the expanded region of the mass spectrum about 154 amu with the readily apparent high-mass trailing distribution of isotopomer peaks. The relative intensities of the peaks following 154 amu is identical to the isotopomer distribution
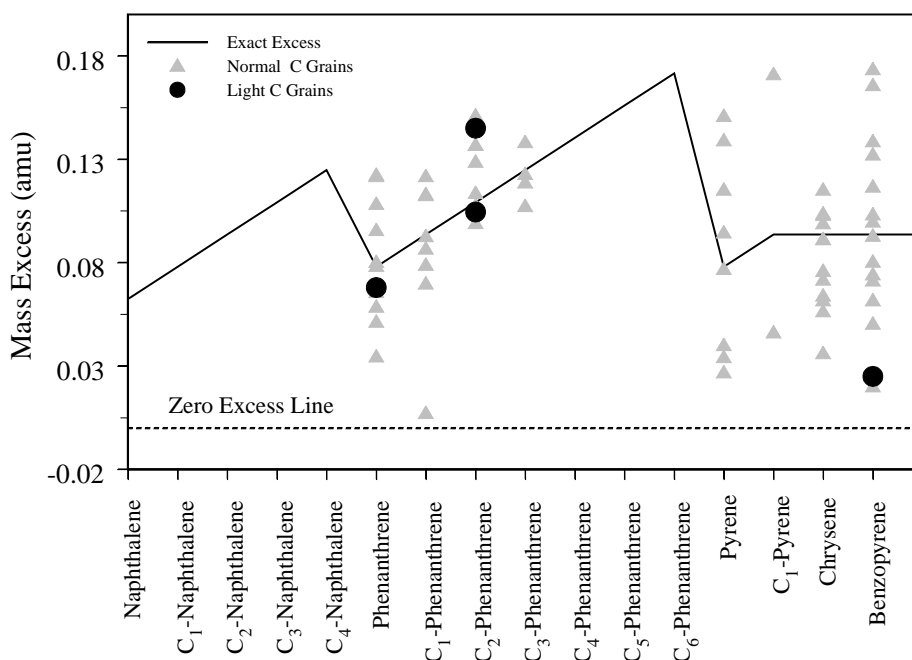
FIG. 9.—Comparison of the exact and measured mass excesses for the dominant molecular species observed in both normal C and light C grains. In all cases the measured mass excesses of molecules from normal C grains are normally distributed about the exact value calculated for the relevant PAH of that mass. This result argues persuasively for the mass assignments of these species as PAHs. Also shown are the measured mass excesses for four molecular species observed in light C grains that show evidence for ^{13}C depletions. The mass excesses measured in these molecules fall within the normal distribution range of the isotopically normal species, supporting their assignments as PAHs.

predicted for this molecule assuming its C isotopic composition is the same as its parent graphite grain. The result needs nevertheless to be interpreted with some caution because of potential molecular interferences at 156 amu arising from C_2-alkyl naphthalene ($C_{12}H_{12}$), which is observed on some other grains. Identification of additional candidate molecules showing ^{13}C enrichments are at present only tentative and cannot be subject to the same rigorous statistical analysis as is the case for ^{13}C-poor grains. In this respect grain M7.25 is unique in that there are generally only a few potential chemical interferences for such simple low-mass PAHs and acenapthalene is not abundant in the μL^2MS spectra of either Murchison or its acid insoluble residue mitigating the effects of isotopic dilution.

Strong circumstantial evidence of dramatic isotopmer enrichment is found in grain K10 ($R = 10$). Figure 12 shows the mass distribution for this ^{13}C-rich grain, the isotopically normal grain M8.54, and Murchison acid residue. Both

K10 and grain M8.54 have comparable integrated total signal intensities but have distinctly different mass envelopes. Grain M8.54 has similarities to the acid residue, with the dominant PAHs being the same in both spectra. Grain K10, in contrast, shows *no* prominent peaks and has a *greater* spectral complexity than any other grain measured in this study. Although not conclusive, this behavior is consistent with what is expected of an extended suite of ^{13}C-enriched PAHs in which each PAH shows a wide distribution of overlapping isotopomer peaks.

Table 1 summarizes the isotopically anomalous molecules identified to date. As previously discussed, the apparently ubiquitous presence of isotopically normal PAHs, compounded with heteroaromatic interferences, has limited the ability to identify isotopically anomalous molecules with those in fortuitously uncrowded spectral regions. Nevertheless, it is still possible to make certain generalizations about the indigenous PAHs. The molecules span a moderate mass range, from 178 to 270 amu, essentially

TABLE 1

ISOTOPICALLY ANOMALOUS MOLECULES IDENTIFIED TO DATE

Grain	R_{grain}	Mass (amu)	$P_N(n_2)$	$R_{molecule}$[a]	Assignment[b]	Structure
M11-15......	1727	178	0.038	215	Phenanthrene	$C_{14}H_{10}$
M11-15......	1727	192	0.012	355	C_1-phenanthrene	$C_{15}H_{12}$
M7-20	648	206	0.00027	311	C_2-phenanthrene	$C_{16}H_{14}$
K25..........	1508	228	0.0018	216	Chrysene	$C_{18}H_{12}$
M11-7	1237	270	0.0035	576	C_3-chrysene	$C_{21}H_{18}$

[a] Since the measured $^{12}C/^{13}C$ for a given molecule is inversely proportional to the number of isotopomer peak ions observed (from 2 to 14 in the molecules listed here), this number has a large uncertainty, and discrepancies with R_{grain} are not unexpected.

[b] In the situation where one or more isomeric PAHs exist at a given mass, mass assignments are based on the isomer that has the highest photoionization cross section at 266 nm. Hence, mass 178 amu is assigned as phenanthrene rather than anthracene.
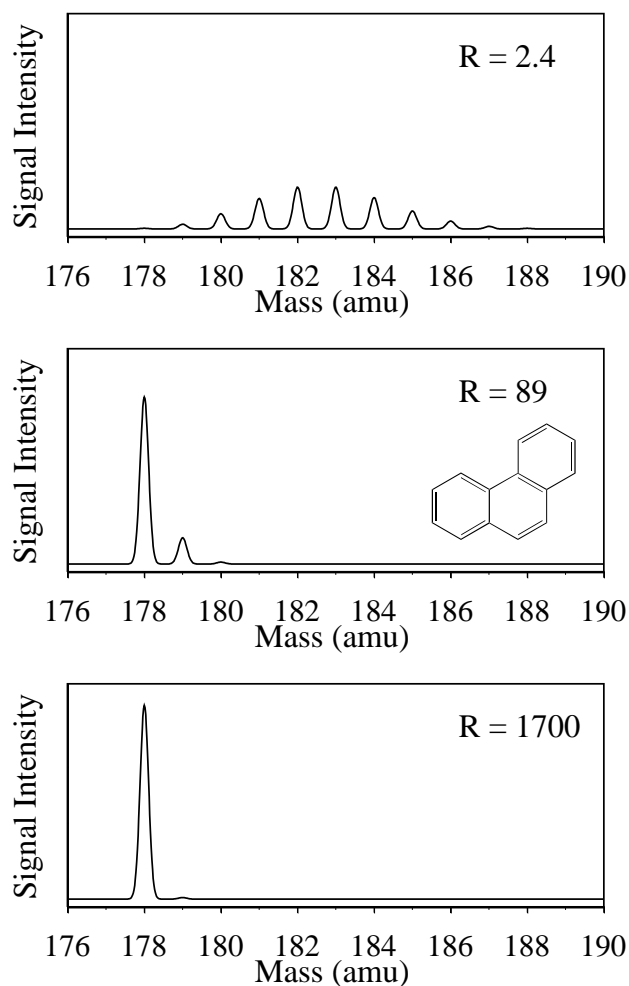
FIG. 10.—Calculated C isotopomer distributions for the molecule phenanthrene at three different values of R (2.4, 89, 1700), representing the two extreme R-values observed in the grains in this study and the solar value.

covering the size range of PAHs observed in other extraterrestrial materials (Clemett 1996). The molecules are diverse and include alkylated species extending up to C_3. However, owing to limited statistics, it is presently impossible to determine if the indigenous PAHs have identical mass patterns in different circumstellar graphite grains.

4. ORIGIN OF THE OBSERVED MOLECULES

We first make the distinction between those PAHs that exhibit correlated isotopic anomalies with their parent graphite grains and that are therefore truly *indigenous* to the grains and those whose isotopic compositions are indistinguishable from the solar value, hereafter referred to as "normal" PAHs. It should be emphasized that although isotopically indistinguishable from solar system materials, many normal PAHs may still have a presolar origin. We note, for reference, that while ensembles of meteoritic microdiamonds also have solar $^{12}C/^{13}C$ values, they are generally believed to be presolar because they are the apparent carriers of the exotic noble gas component Xe-HL (Anders & Zinner 1993 and references therein). In addition, some of the PAHs identified as normal could have a considerable indigenous PAH component, which is obscured in the crowded mass spectrum.
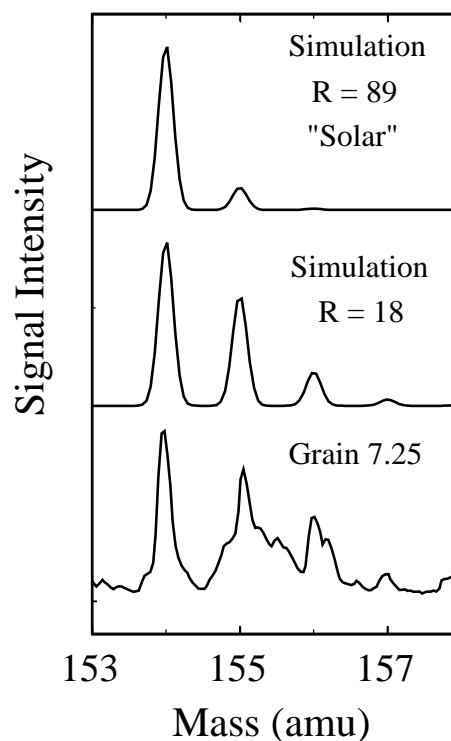

FIG. 11.—Evidence for ^{13}C enriched acenaphthalene in grain 7.25. This grain was measured by ion probe to have a large ^{13}C enrichment ($R = 18$).

The extremely variable mass distributions and relative abundances of the normal PAHs observed from one graphite grain to the next indicate that the normal PAHs are not a unique contaminant introduced during the chemical treatments used to isolate the grains from their parent meteorites. The normal PAHs could have been introduced to the graphite grains at any number of stages in the complex history of the grains. Indeed, the variable nature of the normal PAHs suggests that different processes have been operative on different grains. Although the lack of distinctive isotopic signatures may make it difficult to determine the origins of the normal PAHs, important constraints may emerge from work on the stability and siting of PAHs within the grains.
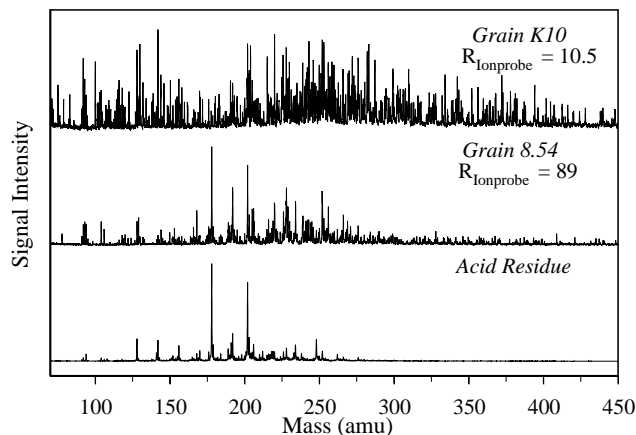

FIG. 12.—Comparison of the PAH spectrum observed from the ^{13}C enriched grain K10 with spectra from an isotopically normal grain and Murchison acid residue.

Although the indigenous PAHs may also have been formed at different stages in the history of the grains, the isotopic linkage between the molecules and the grains provides an important constraint on their formation mechanism.

Certainly one possible origin of the indigenous PAHs is in gas-phase reactions followed by incorporation into the growing graphite grains. TEM studies of circumstellar graphite provide independent, albeit indirect, evidence for the presence of PAHs (Bernatowicz et al. 1996). TEM analysis shows that most grains ($\sim 80\%$) have a distinct nanocrystalline C core surrounded by well-graphitized C. These nanocrystalline C cores usually constitute a significant fraction of the mass of the grains. Electron diffraction studies show that the core material is composed primarily of randomly oriented hexagonal sheets of C atoms with sp^2 bonding (aromatic), typically 3–4 nm in size (graphene). This material can be considered part of a structural continuum, with PAHs representing the small size limit. Indeed, electron diffraction patterns of the core material indicate that there must be a large number of aromatic units less than 1 nm in size, perhaps accounting for as much as 25% of the core material. The authors suggest that the graphene and "PAH-like material" were produced in the gas phase prior to graphite formation, later condensing to provide nucleation centers for further graphite growth.

Bernatowicz et al. (1996) have modeled the formation of graphite in circumstellar atmospheres, providing constraints on the temperature, pressure, and timescale for their growth based on the grain sizes and the presence of internal carbides. They argued that the nanocrystalline C cores formed under conditions of supersaturation in anomalously dense regions of the stellar atmosphere (density clumps) at a temperature of at least 1550 K.

Cherchneff, Barker, & Tielens (1992) have developed a chemical kinetic model for PAH formation in C-rich circumstellar outflows, although with low predicted production rates. While the temperature constraint derived by Bernatowicz et al. (1996) is substantially higher than generally expected for PAH formation (~ 1200 K), Cherchneff, Barker, & Tielens (1991) argue that PAH chemistry is dependent on the PAH's vibrational temperature and not the gas kinetic temperature. Owing to the ability of PAH molecules to rapidly dissipate vibrational energy through fluorescence, the vibrational temperature may be several hundred degrees below the gas kinetic temperature in typical stellar atmosphere conditions. By invoking this "inverse greenhouse effect," PAH formation is expected to commence when the gas kinetic temperature drops to 1500 K, effectively reconciling gas phase PAH formation with the temperature constraints imposed on circumstellar graphite formation. The conditions of high-density supersaturation required for circumstellar graphite grain formation determined by Bernatowicz et al. (1996) are more favorable for PAH production than those assumed by Cherchneff et al. (1991), possibly leading to substantially higher PAH yields in their model.

IR emission features attributed to PAHs are commonly observed in C-rich planetary nebulae, formed from the mass ejected in strong AGB stellar winds (e.g., Cohen et al. 1986). Direct observation of these emission features in the atmospheres of C-rich red giants may be difficult because of the lack of UV photons necessary to induce PAH fluorescence.

Some fraction of the indigenous PAHs observed within the grains may be a product of radiation processing, either while traversing the interstellar medium or during their residence in the presolar molecular cloud. Starukhina et al. (1990) have demonstrated that radiation-induced formation of PAHs in H-saturated graphite under realistic astrophysical conditions is possible. For example, 10 KeV irradiation of H-saturated graphite by H, He, and N ions all lead to the generation of simple PAHs and their alkylated homologs in the top 1000 Å of the exposed graphite surface. For the case of interstellar graphite, we estimate that the total energy deposited in a typical grain by galactic cosmic rays during an assumed 10^7 yr exposure ($> 2 \times 10^{21}$ eV) is sufficient to account for several ppm of PAHs (assuming 100% production efficiency). In reality the actual radiation exposure could be far higher and this is thus a potentially significant process.

Still another process that cannot be excluded is the synthesis of PAHs in solid state reactions resulting from supernova shock wave interactions in the interstellar medium. Indeed, some workers have calculated rather large grain destruction rates from such interactions (e.g., Draine 1995) and under these conditions conversion of a preexisting carbon-hydrogen mixture into PAHs must be considered.

It is conceivable that the indigenous PAHs formed as a result of hydrothermal processing of the graphite grains on their meteorite parent bodies. However, aqueous processes are more likely to be important for transporting PAHs than for producing PAHs and as such should be considered as a potentially significant source of the normal PAHs. These issues may be clarified by comparing the PAHs present in graphite grains extracted from different meteorite classes, which have experienced a range of aqueous and thermal processing.

5. CONCLUDING REMARKS

Several lines of future investigation deserve to be pursued. In this work we have concentrated on searching for positive correlations between the carbon-isotopic composition of PAHs and their parent graphite grains. Further studies should look for potential correlations between subsets of indigenous PAHs and probable stellar origins of the graphite grains as determined by isotopic analysis. An observed correspondence between the nature or abundance of indigenous PAHs and the stellar origin of the parent graphite would leave little doubt that these molecules coformed with the graphite in a circumstellar environment. Potentially powerful constraints on the physical and chemical conditions of circumstellar graphite formation could be provided by complementary TEM analysis of the *same* grains studied by the dual techniques described here. This is not a trivial experiment, but it is possible.

Further progress in understanding the origins of the different PAH species would be greatly helped if some method could be found to physically separate the normal from the indigenous PAHs. This might be achieved, for example, if the indigenous PAHs were more tightly bound to the graphite, allowing for simple heating of the grains to drive off the more easily volatilized normal PAHs. It is also possible that the normal PAHs are more susceptible to organic solvents and the grains could be "cleaned" of the normal component. The indigenous PAHs may very well be concentrated in the nanocrystalline cores common to most graphite grains. It is possible, though admittedly very difficult, to separate the core material from the parent graphite

grains for independent study.

Although we lean to the view that the indigenous PAHs were produced in gas-phase reactions and incorporated into the graphite grains as they were forming, other mechanisms cannot be ruled out. However, the PAHs produced by high-temperature gas-phase reactions should be distinct in their mass distributions and degrees of alkylation from those produced by exposure of graphite to thermal, radiation or aqueous processing. More detailed characterization of the indigenous PAHs, combined with laboratory investigations of analog systems may help determine the origin of these molecules. However, since the molecules produced may be highly dependent on the distribution, nature and abundance of reacting species, *such radiation, heating, and aqueous treatments should be applied to the circumstellar graphite grains themselves.*

REFERENCES

Allamandola, L. J., Tielens, A. G. G. M., & Barker, J. R. 1985, ApJ, 290, L25
———. 1989, ApJS, 71, 733
Amari, S., Anders, E., Virag, A., & Zinner, E. 1990, Nature, 345, 238
Amari, S., Hoppe, P., Zinner, E., & Lewis, R. 1993a, Nature, 365, 806
Amari, S., Lewis R., & Anders E. 1994, Geochim. Cosmochim. Acta, 58, 459
Amari, S., Zinner, E., & Lewis, R. S. 1993b, Meteoritics, 28, 316
Anders, E., & Zinner E. 1993, Meteoritics, 340, 906
Bernatowicz, T., Amari, S., Zinner, E., & Lewis, R. S. 1991, ApJ, 373, L73
Bernatowicz, T., Cowsic, R., Gibbons, P. C., Lodders, K., Fegley, B., Jr., Amari, S., & Lewis, R. S. 1996, ApJ, 472, 760
Bernatowicz, T., Fraundorf, G., Tang, M., Anders, E., Wopenka, B., Zinner, E., & Fraundorf, P. 1987, Nature, 330, 728
Bialkowski, S. E. 1987, Rev. Sci. Instrum., 58, 2338
Bregman, J. D. 1989, in IAU Symp. 135, Interstellar Dust, ed. L. J. Allamandola & A. G. G. M. Tielens (Dordrecht: Kluwer), 109
Carey, W., Zinner, E., Fraundorf, P., & Lewis, R. S. 1987, Meteoritics, 22, 349
Cherchneff, I., Barker, J. R., & Tielens, A. G. G. M. 1991, ApJ, 377, 541
———. 1992, ApJ, 401, 269
Clemett, S. J. 1996, Ph.D. thesis, Stanford Univ.
Clemett, S. J., Maechling, C. R., Zare, R. N., & Alexander, C. M. O'D. 1992, Lunar Planet. Sci., 23, 233
Clemett, S. J., Maechling, C. R., Zare, R. N., Swan, P. D., & Walker, R. M. 1993, Science, 262, 721
Clemett, S. J., & Zare, R. N. 1997, in IAU Symp. 178, Molecules in Astrophysics: Probes and Processes, ed. E. F. van Dishoeck (Dordrecht: Kluwer), 305
Cohen, M., Allamandola, L. J., Tielens, A. G. G. M., Bregman, J., Simpson, J. P., Witteborn, F. C., Wooden, D., & Rank, D. 1986, ApJ, 302, 737
Cronin, J. R., Pizzarello, S., & Cruikshank, D. P. 1988, in Meteorites and the Early Solar System, ed. J. F. Kerridge & M. S. Matthews (Tucson: Univ. Arizona Press), 819
Draine, B. T. 1995, Ap&SS, 233, 111
Geballe, T. R., Lacy, J. H., Persson, S. E., McGregor, P. J., & Soifer, B. T. 1985, ApJ, 292, 500
Hahn, J. H., Zenobi, R., Bada, J. F., & Zare, R. N. 1988, Science, 239, 1523
Hoppe, P., Strebel, R., Eberhardt, P., Amari, S., & Lewis, R. 1994, Lunar Planet. Sci., 25, 563
Huss, G., Fahey, A., Gallino, R., & Wasserberg, G. 1994, ApJ, 430, L81
Kovalenko, L. J., Maechling, C. R., Clemett, S. J., Philippoz, J.-M., Zare, R. N., & Alexander, C. M. O'D. 1992, Anal. Chem., 64, 682

Kroto, H. 1988, Science, 242, 1139
Kroto, H. W., Heath, J. R., O'Brien, S. C., Curl, R. F., & Smalley, R. E. 1985, Nature, 318, 162
Leger, A., & Puget, J. L. 1984, ApJ, 137, L5
Levy, R. L., Grayson, M. A., & Wolf, C. J. 1973, Geocim. Cosmochim. Acta, 37, 467
Lewis, R. S., Tang, M., Wacker, J. F., Anders, E., & Steel, E. 1987, Nature, 326, 160
Maechling, C. R., Clemett, S. J., & Zare, R. N. 1995, Chem. Phys. Lett., 241, 301
Newton, J., Bischoff, A., Arden, J. W., Franchi, I., Geiger, T., Greshake, A., & Pillinger, C. 1995, Meteoritics, 30, 47
Nittler, L. R., Alexander, C. M. O'D., Gao, X., Walker, R. M., & Zinner, E. 1994, Nature, 370, 443
Nittler, L. R., et al. 1995, ApJ, 453, L25
Pappas, D. L., Hurbowchak, D. M., Ervin, M. H., & Winograd, N. 1989, Science, 243, 64
Pering, K. L., & Ponnamperuma, C. 1971, Science, 173, 237
Sagan, C., Khare, B. N., Thompson, W. R., McDonald, G. D., Wing, M. R., Bada, J. L., Vo-Dinh, T., & Arakawa, E. T. 1993, ApJ, 414, 399
Salma, F., Bakes, E. L. O., Allamandola, L. J., & Tielens, A. G. G. M. 1996, ApJ, 458, 621
Shibanov, A. N. 1985, in Laser Analytical Spectroscopy, ed. V. S. Lekokhov (Bristol: Adam Hilger)
Starukhina, L. V., Shkuratov, Yu. G., Kodina, L. A., Ogloblina, A. I., Stankevich, N. P., Peregon, T. I., & Tishchenko, L. P. 1990, Lunar Planet. Sci., 21, 1192
Tang, M., & Anders, E. 1988, Geochim. Cosmochim. Acta, 52, 1235
Thomas, K. L., et al. 1995, Geochim. Cosmochim. Acta, 59, 2797
Wiley, W. C., & McLaren, I. H. 1955, Rev. Sci. Instrum., 26, 1150
Willner, S. P., Soifer, B. T., Russell, R. W., Joyce, R. R., & Gillett, F. C. 1977, ApJ, 217, L121
Winograd, N., Baxter, J. P., & Kimock, F. M. 1982, Chem. Phys. Lett., 82, 591
Zenobi, R., Philippoz, J.-M., Buseck, P. R., & Zare, R. N. 1989, Science, 246, 1026
Zenobi, R., Philippoz, R.-M., Zare, R. N., Wing, M. R., Bada, J. L., & Marti, K. 1992, Geochim. Cosmochim. Acta, 56, 2899
Zenobi, R., & Zare, R. N. 1991, in Advances in Multiphoton Processes and Spectroscopy, vol. 7, ed. S. H. Lin (Singapore: World Scientific), 1
Zinner, E., Tang, M., & Anders, E. 1989, Geochim. Cosmochim. Acta, 53, 3273